Chapter 11
Representative Volume Element Size and Length Scale Identification in Generalised Magneto-Elasticity

Sinan Eraslan, Inna M. Gitman, Mingxiu Xu, Harm Askes, and René de Borst

Abstract A generalised magneto-elastic continuum model with gradients of strain, magnetic field, and piezo-magnetic coupling terms has been discussed in this study. Characteristic length scale parameters, accompanying the higher order components in the model, have been identified in terms of representative volume element (RVE) sizes, in order to introduce the microstructural information to material properties on the macro-level. Following this qualitative definition, a quantitative determination, and the analysis of RVE sizes in different physical phenomena, a RVE and, hence, length-scale enriched generalised gradient magneto-elastic continuum model has been employed in a benchmark numerical example demonstrating the removal of singularities from magnetic and mechanical fields.

Key words: Magnetorheological elastomers · RVE size · Length scale · Generalised magneto-elastic continuum

Sinan Eraslan
The University of Sheffield, Department of Mechanical Engineering, Sheffield, United Kingdom,
e-mail: seraslan1@sheffield.ac.uk

Inna M. Gitman · Harm Askes
University of Twente, Faculty of Engineering Technology, Enschede, The Netherlands,
e-mail: i.m.gitman@utwente.nl, h.askes@utwente.nl

Mingxiu Xu
University of Science and Technology Beijing, Department of Applied Mechanics, Beijing, P.R. China,
e-mail: xumx@ustb.edu.cn

René de Borst
The University of Sheffield, Department of Civil and Structural Engineering, Sheffield, United Kingdom,
e-mail: r.deborst@sheffield.ac.uk

H. Altenbach et al. (eds.), *Sixty Shades of Generalized Continua*,
Advanced Structured Materials 170, https://doi.org/10.1007/978-3-031-26186-2_11

11.1 Introduction

Smart composite materials have been the topic of many research investigations in the last few decades due to being responsive to external stimulus such as temperature, pH, electric or magnetic field [1, 2]. One type of these responsive materials, known as magnetorheological elastomers (MREs), consist of magnetic particles embedded in a silicone-based elastomer, and present a coupling between magnetism and elasticity via the magnetostriction effect [1]-[4]. Magnetostriction is a phenomenon in which a magnetic field leads to a change in shape in ferromagnetic materials. In MREs, particles will exhibit magnetostrictive behaviour when a magnetic field is applied. Thus, forces will be exerted to the polymer matrix and the composite material will deform [3, 5]. This coupling phenomena proposes various potential applications in many engineering fields, including actuators, sensors, vibration isolation and control, sensing of ultrasonic waves, micro beams/plates in micro-electro-mechanical systems (MEMS) and dialysis membranes in biomedical applications [1]-[3], [6]-[8]. Various magnetic materials such as Terfenol-D, cobalt ferrite, certain earth metals and iron alloys can be used as magnetic filler with several alternatives for the elastic matrix such as natural rubber, silicone rubber, vinyl rubber or polyurethane [2, 4, 9, 10].

MREs can be categorised as macroscopically isotropic or anisotropic depending on the particle distribution in the matrix. Polymer and particles are mixed mechanically with some additives, and then the mixture is cured without or with magnetic field to obtain isotropic or anisotropic MREs, respectively [2, 4, 9]. Various reviews have been conducted on the fundamentals of magnetostriction, manufacturing/modelling of MREs, and their applications. Magnetic responsive polymer composites (MRPCs) have been reviewed by Thévenot et al. [2] and Filipcsei et al. [1] by presenting different types of MRPCs, detailed fabrication methods including used products, preparation steps and chemical processes. Progress after 2000 and the current state of those materials have been evaluated by Elhajjar et al. [3] with some examples of different compositions (such as galfenol alloys, cobalt ferrites, Terfenol-D alloys and carbonyl iron). Ekreem et al. [5] explained how magnetostriction occurs and presented measurement procedures of this phenomenon. In this overview, the advantages and disadvantages of the procedures were discussed to conclude the most common and sensitive methods.

Researchers have proposed various microscopic and macroscopic material models of MREs and ferrogels since their introduction in the late 1990s. A microscopic model has been presented by Wood and Camp [10] to study the relationship between physical properties of the ferrogels and features of the microstructure using Monte Carlo computer simulations. These authors demonstrated that it is feasible to control the elastic modulus of the ferrogel by applying a uniform magnetic field to the samples at the gel-formation stage. Another microscopically motivated approach, derived from the continuum formulation of a magneto-mechanical boundary value problem, has been developed by Kalina et al. [11] to study the influence of mechanical preloads on the deformation behaviour of MREs. Attaran et al. [12] presented a macroscopic model to capture the mechanical deformation of ferrogels. They proposed this macroscopic model as a simplified form of a previously developed continuum model, and they demonstrated a good agreement between numerically predicted and experimental results. Further, Raikher and Stolbov [13] have followed a continuum approach for MREs by considering them as a homogeneous and isotropic elastic medium. Besides limitations and drawbacks, the model can present practical and experimentally acceptable results.

It is known that microscopic properties affect the macroscopic behaviour of heterogeneous materials. Therefore, introducing microstructural information in the macroscopic continuum results in a significant improvement in accurately describing and predicting the response of an MRE. Accordingly, a multi-scale approach can be used in the analysis of these materials as various scales have to be studied simultaneously [14]. So called analytical homogenisation is a multi-scale approach in which the material is described as a heterogeneous medium on the micro-level, by considering each component's configuration and constitutive properties explicitly; simultaneously, material is described as homogeneous on the macro-level, and the constants in constitutive relations of the macrostructure appear in the form of effective properties (see, among others [15, 16]). The Representative Volume Element (RVE) approach is typically employed to model the material on the micro-scale. Here, RVE is the smallest part of a material which is large enough to be constitutively valid [15]. The unit cell (representative unit cell, or, indeed an RVE) is considered as input parameter in analytical homogenisation approaches.

On the other hand, several authors have proposed nonlocal continuum theories to include the information from the micro-scale in the macroscopic continuum via additional material constants such as characteristic length scale parameters [8, 16, 17]. It was already shown in [15, 16] that there is a link between the RVE size on the micro-scale and additional characteristic length scale parameters on the macro-scale. The authors have extended the theory to magneto-elasticity, and derived macro-level magneto-elastic constitutive relations enriched with higher-order terms accompanied by characteristic length scale parameters. They also proposed a statistical method to determine the RVE sizes for different phenomena in an MRE material [18]. However, they have not used the determined RVE sizes, and hence identified length scale parameters, in the macro-level magneto-elastic constitutive relations to show the effects of the additional parameters on static magneto-elastic behavior.

The aim of this study is to present the influence of identified length scale parameters in removing mechanical and magnetic singularities by using the determined RVE sizes as model parameters in generalised magneto-elasticy, thereby bridging the gap between RVE-based approaches and generalised/nonlocal continuum approaches. In Sect. 11.2, the macro-level magneto-elastic constitutive formulation with identified length scale parameters and determined RVE sizes will be discussed. In Sect. 11.3, numerical results will be presented for a two-dimensional in-plane problem to remove singularities in mechanical and magnetic fields. Finally, some closing remarks are presented in Sect. 11.4.

11.2 Formulation

Magnetostrictive materials typically exhibit non-linear material behaviour. However, mechanical pre-stresses and bias magnetic fields are generally applied in most applications. These bias conditions allow to use linear piezomagnetic equations to describe the material behaviour. In a static magnetic field (curl-free), the constitutive equations of a linear piezomagnetic medium in classical continuum theory can be given as [8], [18]-[21]

$$\sigma_{ij} = C_{ijkl}\varepsilon_{kl} - Q_{nij}H_n, \qquad B_i = Q_{ikl}\varepsilon_{kl} + \mu_{in}H_n \tag{11.1}$$

with the kinematic relationships

$$\varepsilon_{ij} = \frac{1}{2}(u_{i,j} + u_{j,i}) \text{ and } H_i = -\varphi_{,i} \tag{11.2}$$

where $\boldsymbol{\sigma}$ and $\boldsymbol{B}$ are the stress tensor and the magnetic induction vector, $\boldsymbol{C}$ and $\boldsymbol{Q}$ are the stiffness tensor and the piezomagnetic coupling tensor, $\boldsymbol{\mu}$ is the magnetic permeability, $\boldsymbol{\varepsilon}$ and $\boldsymbol{H}$ are the strain tensor and the magnetic field vector, and $\boldsymbol{u}$ and φ are the displacement field vector and the scalar magnetic potential.

11.2.1 Homogenisation and Macroscopic Characteristic Length Scale Parameters

As discussed above, micro and macro scales are linked to each other by model parameters in a multi-scale framework. The MRE material is considered as heterogeneous to reflect the real structure on the micro-level, but it is modelled as a piezomagnetic material with homogeneous effective material properties and model parameters on the macro-level. The concept of an RVE is used to quantify the micro scale behaviour and, hence, the size of the RVE becomes a model parameter in the multi-scale approach. This approach combines the advantage of computational efficiency with an accurate description of the material behaviour on the macro-level.

In the multi-scale analysis, the macroscopic stress and induction in the MRE can be defined as the volume average of the microscopic counterparts in the RVE:

$$\begin{aligned} \sigma_{ij}^{\mathrm{M}} &= \frac{1}{V_{\mathrm{RVE}}} \int\limits_{V_{\mathrm{RVE}}} \sigma_{ij}^{\mathrm{m}} \mathrm{d}V = \frac{1}{V_{\mathrm{RVE}_1}} \int\limits_{V_{\mathrm{RVE}_1}} C_{ijkl}^{\mathrm{m}} \varepsilon_{kl}^{\mathrm{m}} \mathrm{d}V - \frac{1}{V_{\mathrm{RVE}_2}} \int\limits_{V_{\mathrm{RVE}_2}} Q_{nij}^{\mathrm{m}} H_n^{\mathrm{m}} \mathrm{d}V \\ B_i^{\mathrm{M}} &= \frac{1}{V_{\mathrm{RVE}}} \int\limits_{V_{\mathrm{RVE}}} B_i^{\mathrm{m}} \mathrm{d}V = \frac{1}{V_{\mathrm{RVE}_3}} \int\limits_{V_{\mathrm{RVE}_3}} Q_{ikl}^{\mathrm{m}} \varepsilon_{kl}^{\mathrm{m}} \mathrm{d}V + \frac{1}{V_{\mathrm{RVE}_4}} \int\limits_{V_{\mathrm{RVE}_4}} \mu_{in}^{\mathrm{m}} H_n^{\mathrm{m}} \mathrm{d}V \end{aligned} \tag{11.3}$$

It can initially be assumed that an MRE has different RVEs as given in Eq. (11.3), with V_{RVE_1} and V_{RVE_4} representing purely mechanical and purely magnetic phenomena, while V_{RVE_2} and V_{RVE_3} correspond to coupling phenomena. The superscripts m and M denote the micro and the macro level, respectively.

Next, by using a second-order homogenisation scheme and Eq. (11.3), macroscopic constitutive and governing equations can be derived. These equations include gradients in terms of the RVE sizes to introduce the micro-level information into the macro-level. The associated local coordinate systems are assumed to have their origin at the centre of the RVE. Before applying second-order homogenisation, linearisations of spatially dependent stiffness, strain, coupling, permeability and magnetic field can be presented as

$$\begin{aligned} &C^{\mathrm{m}}_{ijkl} = C^{\mathrm{M}}_{ijkl} + C^{\mathrm{M}}_{ijkl,o}\delta x_o, \quad \varepsilon^{\mathrm{m}}_{kl} = \varepsilon^{\mathrm{M}}_{kl} + \varepsilon^{\mathrm{M}}_{kl,p}\delta x_p, \quad Q^{\mathrm{m}}_{nij} = Q^{\mathrm{M}}_{nij} + Q^{\mathrm{M}}_{nij,o}\delta x_o \\ &H^{\mathrm{m}}_n = H^{\mathrm{M}}_n + H^{\mathrm{M}}_{n,p}\delta x_p, \quad \mu^{\mathrm{m}}_{in} = \mu^{\mathrm{M}}_{in} + \mu^{\mathrm{M}}_{in,o}\delta x_o \end{aligned} \tag{11.4}$$

The constitutive relation for the macroscopic stress and magnetic induction (Eq. (11.3)) can be rewritten as

$$\begin{aligned} \sigma^{\mathrm{M}}_{ij} =& \frac{1}{V_{\mathrm{RVE}_1}} \int\limits_{V_{\mathrm{RVE}_1}} \left(C^{\mathrm{M}}_{ijkl}\varepsilon^{\mathrm{M}}_{kl} + C^{\mathrm{M}}_{ijkl}\varepsilon^{\mathrm{M}}_{kl,p}\delta x_p + C^{\mathrm{M}}_{ijkl,o}\varepsilon^{\mathrm{M}}_{kl}\delta x_o + C^{\mathrm{M}}_{ijkl,o}\varepsilon^{\mathrm{M}}_{kl,p}\delta x_o\delta x_p \right) \mathrm{d}V \\ &- \frac{1}{V_{\mathrm{RVE}_2}} \int\limits_{V_{\mathrm{RVE}_2}} \left(Q^{\mathrm{M}}_{nij}H^{\mathrm{M}}_n + Q^{\mathrm{M}}_{nij}H^{\mathrm{M}}_{n,p}\delta x_p + Q^{\mathrm{M}}_{nij,o}H^{\mathrm{M}}_n\delta x_o + Q^{\mathrm{M}}_{nij,o}H^{\mathrm{M}}_{n,p}\delta x_o\delta x_p \right) \mathrm{d}V \\ B^{\mathrm{M}}_i =& \frac{1}{V_{\mathrm{RVE}_3}} \int\limits_{V_{\mathrm{RVE}_3}} \left(Q^{\mathrm{M}}_{ikl}\varepsilon^{\mathrm{M}}_{kl} + Q^{\mathrm{M}}_{ikl}\varepsilon^{\mathrm{M}}_{kl,p}\delta x_p + Q^{\mathrm{M}}_{ikl,o}\varepsilon^{\mathrm{M}}_{kl}\delta x_o + Q^{\mathrm{M}}_{ikl,o}\varepsilon^{\mathrm{M}}_{kl,p}\delta x_o\delta x_p \right) \mathrm{d}V \\ &+ \frac{1}{V_{\mathrm{RVE}_4}} \int\limits_{V_{\mathrm{RVE}_4}} \left({\mu^{\mathrm{M}}}_{in}H^{\mathrm{M}}_n + \mu^{\mathrm{M}}_{in}H^{\mathrm{M}}_{n,p}\delta x_p + \mu^{\mathrm{M}}_{in,o}H^{\mathrm{M}}_n\delta x_o + \mu^{\mathrm{M}}_{in,o}H^{\mathrm{M}}_{n,p}\delta x_o\delta x_p \right) \mathrm{d}V \end{aligned} \tag{11.5}$$

In Eq. (11.5), $C^{\mathrm{M}}_{ijkl}, \varepsilon^{\mathrm{M}}_{kl}, Q^{\mathrm{M}}_{nij}, Q^{\mathrm{M}}_{ikl}, \mu^{\mathrm{M}}_{in}$ and H^{M}_n can be taken out of the integral since they are the values at the centre of the RVEs. Assuming a square RVE with its centre acting as origin of a Cartesian coordinate system, the linear terms of δx cancel as they consist of odd functions integrated over a symmetric domain. The quadratic terms are integrated by parts as follows

$$\begin{aligned} \int\limits_{V_{\mathrm{RVE}_1}} C^{\mathrm{M}}_{ijkl,o}\varepsilon^{\mathrm{M}}_{kl,p}\delta x_o\delta x_p \mathrm{d}V =& \int\limits_S C^{\mathrm{M}}_{ijkl}\varepsilon^{\mathrm{M}}_{kl,p}n_o\delta x_o\delta x_p \mathrm{d}S - \int\limits_{V_{\mathrm{RVE}_1}} \left(C^{\mathrm{M}}_{ijkl}\varepsilon^{\mathrm{M}}_{kl,op}\delta x_o\delta x_p \right. \\ &\left. + C^{\mathrm{M}}_{ijkl}\varepsilon^{\mathrm{M}}_{kl,p}\delta x_{o,o}\delta x_p + C^{\mathrm{M}}_{ijkl}\varepsilon^{\mathrm{M}}_{kl,p}\delta x_o\delta x_{p,o} \right) \mathrm{d}V \\ \int\limits_{V_{\mathrm{RVE}_2}} Q^{\mathrm{M}}_{nij,o}H^{\mathrm{M}}_{n,p}\delta x_o\delta x_p \mathrm{d}V =& \int\limits_S Q^{\mathrm{M}}_{nij}H^{\mathrm{M}}_{n,p}n_o\delta x_o\delta x_p \mathrm{d}S - \int\limits_{V_{\mathrm{RVE}_2}} \left(Q^{\mathrm{M}}_{nij}H^{\mathrm{M}}_{n,op}\delta x_o\delta x_p \right. \\ &\left. + Q^{\mathrm{M}}_{nij}H^{\mathrm{M}}_{n,p}\delta x_{o,o}\delta x_p + Q^{\mathrm{M}}_{nij}H^{\mathrm{M}}_{n,p}\delta x_o\delta x_{p,o} \right) \mathrm{d}V \\ \int\limits_{V_{\mathrm{RVE}_3}} Q^{\mathrm{M}}_{ikl,o}\varepsilon^{\mathrm{M}}_{kl,p}\delta x_o\delta x_p \mathrm{d}V =& \int\limits_S Q^{\mathrm{M}}_{ikl}\varepsilon^{\mathrm{M}}_{kl,p}n_o\delta x_o\delta x_p \mathrm{d}S - \int\limits_{V_{\mathrm{RVE}_3}} \left(Q^{\mathrm{M}}_{ikl}\varepsilon^{\mathrm{M}}_{kl,op}\delta x_o\delta x_p \right. \\ &\left. + Q^{\mathrm{M}}_{ikl}\varepsilon^{\mathrm{M}}_{kl,p}\delta x_{o,o}\delta x_p + Q^{\mathrm{M}}_{ikl}\varepsilon^{\mathrm{M}}_{kl,p}\delta x_o\delta x_{p,o} \right) \mathrm{d}V \end{aligned}$$

$$\int\limits_{V_{\mathrm{RVE}_4}} \mu^{\mathrm{M}}_{in,o} H^{\mathrm{M}}_{n,p} \delta x_o \delta x_p \mathrm{d}V = \int\limits_{S} \mu^{\mathrm{M}}_{in} H^{\mathrm{M}}_{n,p} n_o \delta x_o \delta x_p \mathrm{d}S - \int\limits_{V_{\mathrm{RVE}_4}} \Big(\mu^{\mathrm{M}}_{in} H^{\mathrm{M}}_{n,op} \delta x_o \delta x_p + \mu^{\mathrm{M}}_{in} H^{\mathrm{M}}_{n,p} \delta x_{o,o} \delta x_p + \mu^{\mathrm{M}}_{in} H^{\mathrm{M}}_{n,p} \delta x_o \delta x_{p,o} \Big) \mathrm{d}V \tag{11.6}$$

Assuming periodic boundary conditions, the boundary integrals vanish and the last two terms in each of Eq. (11.6) vanish since they consist of odd functions. Furthermore, the integrals with $\delta x_o \delta x_p$ can be evaluated as

$$\int\limits_{\mathrm{V}_{\mathrm{RVE_i}}} \delta x_o \delta x_p \mathrm{d}V = \int\limits_{-\frac{L_i}{2}}^{\frac{L_i}{2}} \int\limits_{-\frac{L_i}{2}}^{\frac{L_i}{2}} \int\limits_{-\frac{L_i}{2}}^{\frac{L_i}{2}} \delta x_o \delta x_p \mathrm{d}x_1 \mathrm{d}x_2 \mathrm{d}x_3 = \frac{1}{12} L_i^5 \delta_{op} \quad (i = 1,2,3,4) \tag{11.7}$$

where δ_{op} is the Kronecker delta, $V_{\mathrm{RVE}_i} = L_i^3$ and L_i is the size of the i^{th} RVE.

The piezomagnetic macroscopic constitutive equations with gradients of strain, magnetic field, and magneto-mechanical coupling terms can thus be expressed as

$$\begin{aligned} \sigma^{\mathrm{M}}_{ij} &= C^{\mathrm{M}}_{ijkl} \left(\varepsilon^{\mathrm{M}}_{kl} - \frac{L_1^2}{12} \varepsilon^{\mathrm{M}}_{kl,pp} \right) - Q^{\mathrm{M}}_{nij} \left(H^{\mathrm{M}}_n - \frac{L_2^2}{12} H^{\mathrm{M}}_{n,pp} \right) \\ B^{\mathrm{M}}_i &= Q^{\mathrm{M}}_{ikl} \left(\varepsilon^{\mathrm{M}}_{kl} - \frac{L_3^2}{12} \varepsilon^{\mathrm{M}}_{kl,pp} \right) + \mu^{\mathrm{M}}_{in} \left(H^{\mathrm{M}}_n - \frac{L_4^2}{12} H^{\mathrm{M}}_{n,pp} \right) \end{aligned} \tag{11.8}$$

As seen in Eq. (11.8), new gradient terms, accompanied with multipliers L_i, appear in addition to the material coefficients of the macroscopic constitutive equations. It can be seen that Eq. (11.8) follows the structure of the gradient enriched piezomagnetic model proposed by Xu et. al [8], and written in terms of phenomenological parameters ℓ_i:

$$\begin{aligned} \sigma_{ij} &= C_{ijkl} \left(\varepsilon_{kl} - \ell_1^2 \varepsilon_{kl,mm} \right) - q_{ijk} \left(H_k - \ell_2^2 H_{k,mm} \right) \\ B_i &= q_{ijk} \left(\varepsilon_{jk} - \ell_3^2 \varepsilon_{jk,mm} \right) + \mu_{ij} \left(H_j - \ell_4^2 H_{j,mm} \right) \end{aligned} \tag{11.9}$$

Comparing Eqs. (11.8) and (11.9), it can be seen that the link between phenomenological parameters, representing internal characteristic length scale parameters ℓ_i, and RVE sizes L_i can be established as follows: $\ell_i^2 = L_i^2/12$.

11.2.2 Determination of RVE Sizes and Identification of Characteristic Length Scale Parameters

In [18], Eqs. (11.3-11.8) were derived to motivate the determination of the RVE sizes. The detailed methodology to determine the RVE size for magneto-elastic material has been presented in the previous study of the authors [18], however the main steps and results of this analysis will be summarised here. The methodology consists of a statistical numerical analysis of a heterogeneous material, undergoing mechanical and magnetic loading via prescribed values of the displacement $\boldsymbol{u}$ and the magnetic potential φ (see Fig. 11.1a). Boundary value problems are solved for multiple realisations of unit cells (see Fig. 11.1b). Resulting values of stresses and magnetic induction are then averaged over a unit cell. A statistical analysis is then performed and the coefficient of variation is compared with a desired accuracy (97% in our case). If the desired accuracy is reached, the current unit cell can be considered representative (i.e. the RVE is found); otherwise the unit cell size is increased (see Fig. 11.1c) and the procedure is repeated for the new larger unit cell size.

As mentioned above, the MRE material, used in this study, consists of circular magnetic inclusions (where a uniform distribution of 100–300 μm in diameter is assumed) and a non-magnetisable polymer matrix; the material parameters of the constituents are presented in Table 11.1. Two hundred different realisations of each unit cell size (ranging from 0.5 to 2.5 mm) have been analysed and the coefficient of

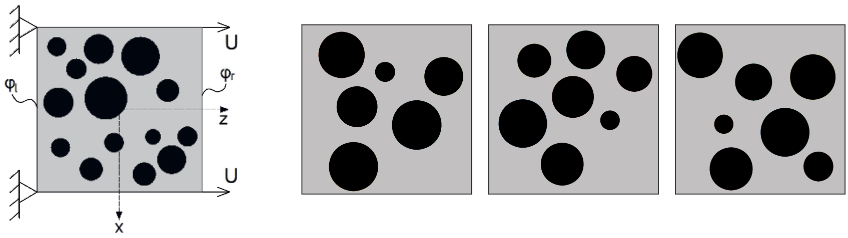

(a) Boundary value problem of a unit cell on micro level

(b) Different realisations of the unit cell (size 1x1 mm^2).

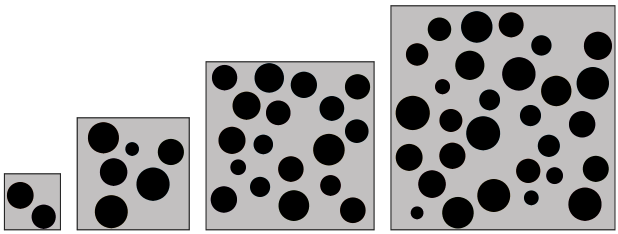

(c) Different sizes of unit cells (from left to right: 0.5x0.5 mm^2, 1x1 mm^2, 1.5x1.5 mm^2, 2x2 mm^2).

Fig. 11.1: Determination of RVE size [18].

Table 11.1: Material properties of magnetic inclusions and polymer matrix.

	C_{11}	C_{13}	C_{33}	C_{55}	Q_{31}	Q_{33}	Q_{15}	μ_{11}	μ_{33}
Terfenol-D [22]	35	23	46	4	-32.5	195	68.75	8.9	1.8
Polymer [23]	7.8	4.7	7.8	1.6	0	0	0	μ_0	μ_0

C_{ij} in GPa, Q_{ij} in N/Am, μ_{ij} in 10^{-6}N/A^2. ($\mu_0 = 4\pi 10^{-6}$ N/A^2)

variation, which is a statistical measure of relative variability, has been calculated for each unit cell size. These coefficients have been compared to the value of 0.03 (i.e. requiring 97% accuracy), and, hence, lower bounds of the RVE sizes (L_i) have been defined (see Fig. 11.2).

For an MRE material, the authors have demonstrated that lower bounds of the RVE sizes can be defined by following the proposed statistical analysis. As can be seen from Fig. 11.2, for the analysed MRE material, the difference between the coupling RVE sizes L_2 and L_3 is negligible in line with thermodynamic consistency requirements, while RVE sizes L_1 and L_4 are clearly smaller and different. According to numerical results, it can be seen that the largest determined RVE size for L_2 and L_3 also covers the lower bound condition for L_1 and L_4. Therefore, it can be concluded that it is sufficient to use only these largest sizes for practical purposes and set $L_1 = L_2 = L_3 = L_4 = \max(L_i) \equiv L$ to introduce the magneto-elastic information from micro-level.

Eventually, the field equations of the problem on the macro scale can be obtained by combining the kinematic relations, balance equations and constitutive equations:

$$\varepsilon^{\mathrm{M}}_{ij} = \frac{1}{2}(u^{\mathrm{M}}_{i,j} + u^{\mathrm{M}}_{j,i}) \quad \text{and } H^{\mathrm{M}}_i = -\varphi^{\mathrm{M}}_{,i} \tag{11.10}$$

$$\sigma^{\mathrm{M}}_{ij,j} = 0 \quad \text{and } B^{\mathrm{M}}_{i,i} = 0 \tag{11.11}$$

where u^{M}_i is the displacement field and φ^{M} is the scalar magnetic potential on the macro-level. The governing equations in terms of the primary unknowns $\boldsymbol{u}$ and φ are

$$\begin{aligned} C^{\mathrm{M}}_{ijkl}\left(u^{\mathrm{M}}_{k,jl} - \frac{L^2}{12}u^{\mathrm{M}}_{k,jlpp}\right) + Q^{\mathrm{M}}_{nij}\left(\varphi^{\mathrm{M}}_{,jn} - \frac{L^2}{12}\varphi^{\mathrm{M}}_{,jnpp}\right) = 0 \\ Q^{\mathrm{M}}_{ikl}\left(u^{\mathrm{M}}_{k,il} - \frac{L^2}{12}u^{\mathrm{M}}_{k,ilpp}\right) - \mu^{\mathrm{M}}_{in}\left(\varphi^{\mathrm{M}}_{,in} - \frac{L^2}{12}\varphi^{\mathrm{M}}_{,inpp}\right) = 0 \end{aligned} \tag{11.12}$$

with L chosen as the largest of the four RVE sizes as discussed above. In the previous study, the authors have not addressed the application of macro-level governing

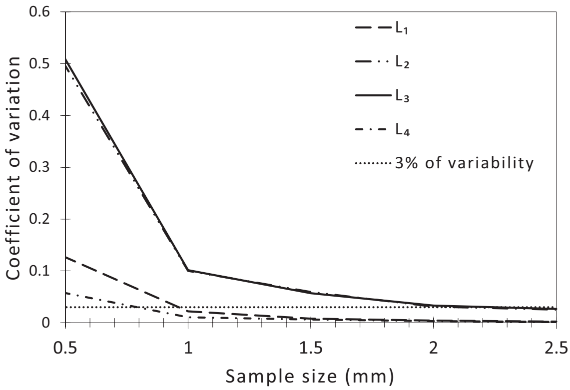

Fig. 11.2 Convergence of the results [18]

equations with identified length scale parameters in terms of RVE size. Here, by using the finite element implementation given in [8], the determined RVE sizes can be used instead of predefined phenomenological length scale parameters in a generalised magnetoelasticity example.

11.3 Numerical Results and Discussion

In this section, the standard benchmark numerical example, demonstrating the removal of singularities in mechanical and magnetic fields, will be analysed to demonstrate the performance of the model. The detailed finite element implementation of gradient enriched piezomagnetic continuum model for in-plane problems has been presented in [8]. For this, the authors extended the Ru-Aifantis approach to gradient magneto-elasticity by considering only one phenomenological length scale parameter in their model (Eq. (11.9)) (see [8] for the details of FEM formulation and in particular the $\boldsymbol{\varepsilon}\&\boldsymbol{H}$-RA approach described therein).

In the numerical example, a homogeneous MRE plate was modelled on the macro-scale with the effective properties (Table 11.2), and external loadings were applied as shown in Fig. 11.3. The plate is polarized along the x-direction with a uniform load $\boldsymbol{q}$ = 10 MPa and magnetic field $\boldsymbol{H}_o$ = 100 A/m. As discussed, it was assumed that $L_1 = L_2 = L_3 = L_4 \equiv L$ in Eq. (11.12), and L is the size of the RVE determined as 2.3 mm (see Fig. 11.2). The crack in the model has been considered as an inclusion with vacuum permeability and zero values for elastic constants, piezomagnetic constants and RVE size L. Figure 11.4 presents the distributions of $\boldsymbol{\varepsilon}$ and

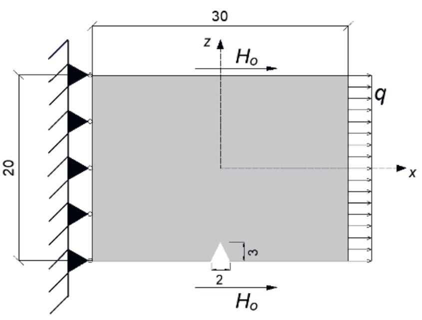

Fig. 11.3 MRE Plate with a crack (Units: mm and thickness = 5 mm)

Table 11.2: Effective material properties of MRE plate.

	C_{11}	C_{13}	C_{33}	C_{55}	Q_{31}	Q_{33}	Q_{15}	μ_{11}	μ_{33}
MRE Plate [8]	31.1	15.2	35.6	13.6	156.8	108.3	-60.9	5.4	5.4

C_{ij} in GPa, Q_{ij} in N/Am, μ_{ij} in 10^{-6}N/A^2

$\boldsymbol{H}$ components in the x-direction around the crack tip. To investigate the effectiveness

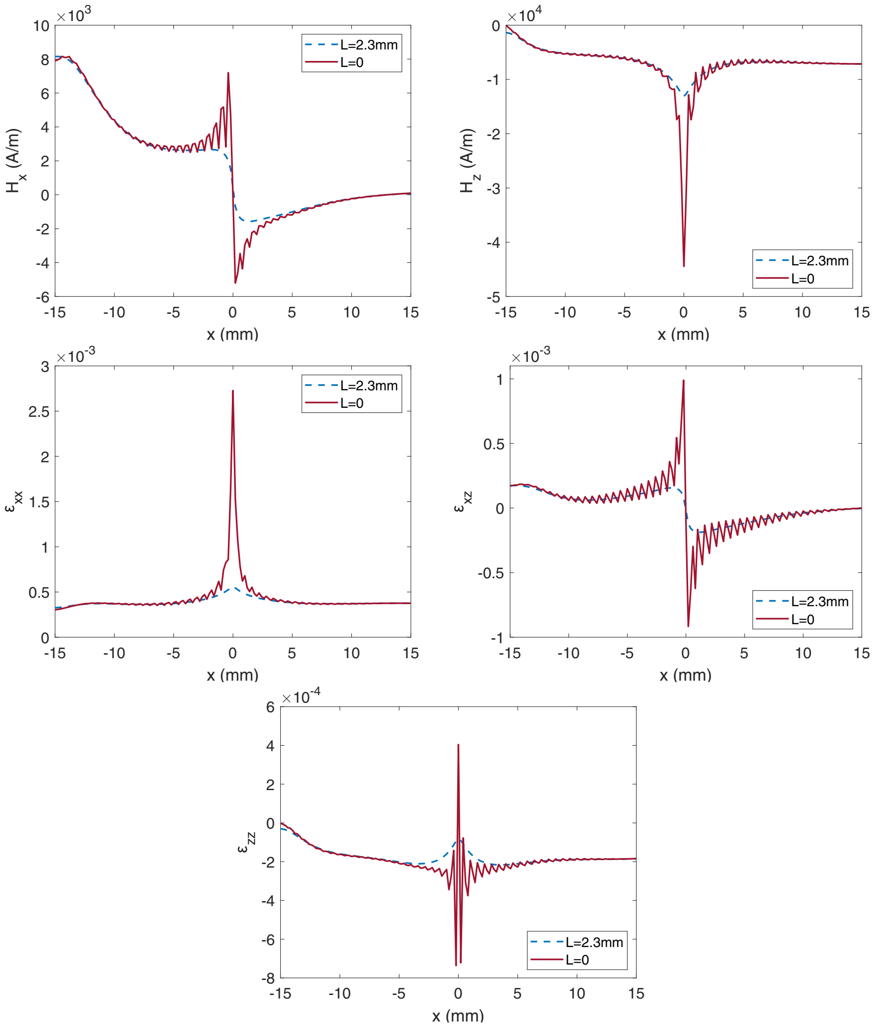

Fig. 11.4: $\boldsymbol{\varepsilon}$ and $\boldsymbol{H}$ distributions along x-axis based on $\boldsymbol{\varepsilon}\&\boldsymbol{H}$-RA approach.

of the gradient formulation, two different cases have been considered: one with length scale $\ell^2 = L_{\mathrm{RVE}}^2/12$ with the RVE size 2.3 mm that considers the gradient dependence, and the other with the length scale $\ell_i = 0$ that represents classical magneto-elasticity in which the microstructural information is absent. It can be seen (Fig. 11.4) that using the gradient enhanced, RVE-based magneto-elasticity formulation can effectively remove the singularities of all $\boldsymbol{\varepsilon}$ and $\boldsymbol{H}$ components, while singularities appear at the crack tip for the classical formulation.

11.4 Conclusions

In this study, an in-plane problem has been addressed by using the previously developed piezo-magnetic continuum model that includes gradients of strain, magnetic field and piezo-magnetic coupling accompanied by characteristic length scale parameter found in terms of RVE size. With this generalised magneto-elastic continuum model, a solution scheme is formulated and implemented based on the finite element method and the Ru-Aifantis theorem adopted from the study by Xu et al. [8]. In the continuum model, representative volume elements (RVEs) have been defined and included to introduce the microstructural information into the macroscopic behaviour of the material. By using the determined model parameter RVE size L, it was observed that the singularities can be removed in mechanical and magnetic fields for a homogenised MRE plate on the macro scale.

Acknowledgements This work was supported by International Graduate Education Scholarship (YLSY) programme funded by The Ministry of National Education of Türkiye.

References

[1] Filipcsei G, Csetneki I, Szilágyi A, Zrínyi M (2007) Magnetic Field-Responsive Smart Polymer Composites, In: Oligomers - Polymer Composites - Molecular Imprinting. Advances in Polymer Science, Vol 206, pp 137-189, Springer, Berlin, Heidelberg.
[2] Thévenot J, Oliveira H, Sandre O, Lecommandoux S (2013) Magnetic responsive polymer composite materials, Chem. Soc. Rev. **42**:7099-7116.
[3] Elhajjar R, Law CT, Pegoretti A (2018) Magnetostrictive polymer composites: Recent advances in materials, structures and properties, Progress in Materials Science **97**:204-229.
[4] Liu T, Xu Y (2019) Magnetorheological elastomers: Materials and applications, In: Xufeng Dong, editor, Smart and Functional Soft Materials, chapter 4. IntechOpen, Rijeka.
[5] Ekreem NB, Olabi AG, Prescott T, Rafferty A, Hashmi MSJ (2007) An overview of magnetostriction, its use and methods to measure these properties, Journal of Materials Processing Technology **191**(1):96-101.
[6] Davis LC (1999) Model of magnetorheological elastomers, Journal of Applied Physics **85**(6):3348-3351.
[7] Liu TY, Chan TY, Wang KS, Tsou HM (2015) Influence of magnetic nanoparticle arrangement in ferrogels for tunable biomolecule diffusion, RSC Adv. **5**:90098-90102.
[8] Xu M, Gitman IM, Askes H (2019) A gradient-enriched continuum model for magneto-elastic coupling: Formulation, finite element implementation and in-plane problems, Computers and Structures **212**:275-288.

[9] Bastola AK, Hoang VT, Li L (2017) A novel hybrid magnetorheological elastomer developed by 3d printing, Materials Design **114**:391-397.

[10] Wood DS, Camp PJ (2011) Modeling the properties of ferrogels in uniform magnetic fields, Phys. Rev. E **83**:011402.

[11] Kalina KA, Metsch P, Kästner M (2016) Microscale modeling and simulation of magnetorheological elastomers at finite strains: A study on the influence of mechanical preloads, International Journal of Solids and Structures **102-103**:286-296.

[12] Attaran A, Brummund J, Wallmersperger T (2017) Modeling and finite element simulation of the magneto-mechanical behavior of ferrogels, Journal of Magnetism and Magnetic Materials **431**:188-191.

[13] Raikher YL, Stolbov OV (2008) Numerical modeling of large field-induced strains in ferroelastic bodies: a continuum approach, Journal of Physics: Condensed Matter **20**(20):204126.

[14] Gitman IM, Askes H, Sluys LJ (2004) Representative volume size as a macroscopic length scale parameter. Fracture Mechanics for Concrete and Concrete Structures, 1:483-491.

[15] Gitman IM (2006) Representative volumes and multi-scale modelling of quasi-brittle materials, Doctoral thesis, Technische Universiteit Delft.

[16] Gitman IM, Askes H, Aifantis EC (2007) Gradient elasticity with internal length and internal inertia based on the homogenisation of a representative volume element, Journal of the Mechanical Behavior of Materials **18**(1):1-16.

[17] Ke L, Wang Y, Yang J, Kitipornchai S (2014) Free vibration of size-dependent magneto-electro-elastic nanoplates based on the nonlocal theory, Acta Mechanica Sinica **30**:516-525.

[18] Eraslan S, Gitman IM, Askes H, de Borst R (2022) Determination of representative volume element size for a magnetorheological elastomer, Computational Materials Science **203**:111070.

[19] Lan M, Wei P (2014) Band gap of piezoelectric/piezomagnetic phononic crystal with graded interlayer, Acta Mechanica **225**:1779–1794.

[20] Mane H (2019) Mathematical Modeling and Numerical Simulation of Magnetoelastic Coupling, Doctoral thesis, Technische Universität Kaiserslautern.

[21] Pang Y, LiuJ, Wang Y, Fang D (2008) Wave propagation in piezoelectric/piezomagnetic layered periodic composites, Acta Mechanica Solida Sinica **21**:483-490.

[22] Claeyssen F, Lhermet N, Barillot F, Le Letty R (2006) Giant dynamic strains in magnetostrictive actuators and transducers, ISAGMM 2006 CONF.

[23] Wang YZ, Li FM, Huang WH, Jiang X, Wang YS, Kishimoto K (2008) Wave band gaps in two-dimensional piezoelectric/piezomagnetic phononic crystals, International Journal of Solids and Structures **45**:4203-4210.